Informes de la Construcción
Vol. 75, 572, e521
octubre-diciembre 2023
ISSN-L: 0020-0883
https://doi.org/10.3989/ic.6273

Research on fatigue vulnerable details of cross beam joints after reinforcement for steel truss bridges

Investigación sobre la debilidad por fatiga de los nodos de vigas transversales antes y después del refuerzo del puente de acero en celosía

Tan Jinhua(*), Jiang Youwei(**), Li Yueguang(***), Liu Yang(****)

ABSTRACT

In this research, fatigue tests on full-size specimens are conducted for a steel cross-beam joint before and after reinforcement. Combined with a three-dimensional (3D) numerical simulation, the 3D stress parameters, and their redistribution rules study anew with a web crack and new crack initiation locations and fatigue weakness details are predicted. The research results include the following: 1) The empirical formula parameter m of the Z-axis stress for the new crack tip is approximately 0.05. 2) The fatigue performance of the web's new crack tips is significantly improved by bolting reinforced steel plates, the stress range is reduced by 60%–98.78%, and the original crack stops growing in size. The health monitoring system can choose the predicted weak details as valid monitoring points so that the fatigue damage can be intelligently perceived after the reinforcement of steel bridges.

Keywords*: bridge engineering; fatigue details; finite element simulation; fatigue tests; three-dimensional stress; crack initiation.*

RESUMEN

En este estudio, la prueba de fatiga de una muestra a gran escala antes y después del refuerzo se llevó a cabo en la junta de viga transversal de un puente de acero. Combinado con la simulación numérica 3D, se estudiaron los parámetros de tensión 3D y las leyes de redistribución de las redes agrietadas, y se predijeron nuevas ubicaciones de grietas y detalles débiles por fatiga. Los resultados muestran que el refuerzo de la placa de acero atornillada puede mejorar la resistencia a la fatiga de la viga, y la amplitud de tensión de la punta de grieta de la placa de banda se puede reducir en más del 60%. Los puntos de monitoreo y medición se pueden establecer en los detalles débiles de la predicción, de modo que el daño por fatiga en el funcionamiento del puente de acero en la etapa posterior del refuerzo se encuentre en un estado de percepción inteligente.

Palabras clave: ingeniería de puentes; detalles de fatiga; simulación de elementos finitos; ensayos de fatiga; tensión tridimensional; iniciación del crack.

(*) Ph.D. Associate professor. Wuhan University of Technology, Wuhan (China).
(**) M.S. Wuhan University of Technology, Wuhan (China).
(***) Ph.D. Associate professor. Wuhan University of Technology, Wuhan (China).
(****) M.S. Wuhan University of Technology, Wuhan (China).
Persona de contacto/*Corresponding author*: jiangyouwei304@gmail.com (Jiang Youwei)
ORCID: http://orcid.org/0000-0003-0946-1535 (T. Jinhua); https://orcid.org/0000-0003-3646-2015 (J. Youwei); https://orcid.org/0000-0001-7338-5093 (L. Yueguang); https://orcid.org/0000-0001-7802-5214 (L. Yang)

Cómo citar este artículo/*Citation:* Tan Jinhua, Jiang Youwei, Li Yueguang, Liu Yang (2023). Research on fatigue vulnerable details of cross beam joints after reinforcement for steel truss bridges. *Informes de la Construcción,* 75(572): e521. https://doi.org/10.3989/ic.6273

Recibido/*Received*: 13/08/2022
Aceptado/*Accepted*: 19/10/2023
Publicado on-line/*Published on-line*: 12/12/2023

1. INTRODUCTION

Fatigue cracking is common in many old steel bridges built in China in the last century. The longest crack detected at the beam joints of steel truss bridges in this research program is 230 mm (1). This makes the fatigue crack reinforcement of a steel beam an important research topic for bridge workers around the world. However, the fatigue problem is affected by many complex factors. The three-dimensional stress state of structures, the formation and propagation mechanisms of multi-fatigue cracks, and their simulation are still some of the major challenges faced by researchers around the world.

Many scholars have predicted the positions of fatigue crack formation in steel truss bridges, Ju Xiao-chen took the I-beam web of a steel bridge as his research object and predicted the fatigue crack propagation behavior with the displacement extrapolation method combined with the maximum energy release rate method (2). Gao Wei studied the rationality of the fatigue force of a steel plate girder bridge joint plate based on the empirical formula and proposed the prediction force model (3). Qu Yu deeply explored the mechanism of the out-of-plane deformation and fatigue cracks in two adjacent openings of a diaphragm in the range of a wheel trace under a load (4). Wang Chun-sheng analyzed the static and dynamic propagation behavior of fatigue-sensitive cracks in detail through the numerical fracture mechanics model of a steel bridge based on the extended finite element method (5). Zhu Jin-song proposed a simulation method and the fatigue crack propagation rules for an orthotropic steel bridge deck based on the finite element model of a real bridge (6). Huang Yun investigated the fatigue problem starting from a crack at the weld root position and proved the propagation characteristics of the fatigue crack using fatigue tests and the fracture mechanics numerical simulation method (7). Liu Yi-ming established a numerical simulation method of three-dimensional crack propagation in the parts of orthotropic steel bridge panels vulnerable to fatigue based on the linear elastic fracture theory (8). Chen Wei-zhen analyzed various factors affecting the fatigue life of welded joints and provided a crack closure model based on the Dugdale model (9). Zhang Ning proposed a fatigue damage assessment method for long-span steel bridges based on meso-damage mechanics (10). Lv Zhilin proposed a simplified test model for a diaphragm in steel beams and investigated the minimum section of an arc-shaped incision in the diaphragm (11).

Wang Teng proposed the probability prediction method using a Monte Carlo integral (12). Nagarajappa, N. predicted the fatigue crack growth behavior for a standard load spectrum (13). Li Menghan proposed a residual fatigue life prediction model for crack growth without considering different stress ratios (14). Bingjie Xiao determined that the crack number density theory could be used as an effective tool for life prediction (15). Robert W proposed a method for estimating crack growth in austenitic steel (16). Ankang Cheng established a fatigue crack growth prediction model suitable for both small-range yield and non-small-range yield conditions (17). Ankang Cheng established a fatigue crack growth prediction model based on the energy principle (18). Zhiping Qiu proposed a disturbance order method for fatigue crack growth prediction considering the initial crack length error (19). M N M Husnain predicted fatigue crack growth from the perspective of damage tolerance (20). Jesper Sundqvist used a numerical simulation method to prove that residual stress had a strong influence on fatigue behavior and fatigue life (21). Amin S. Azar used electron backscatter diffraction to analyze the fatigue crack growth in the weld of high-strength steel under cyclic loads in the plastic zone (22).

In summary, many scholars have performed a large amount of research on the crack growth of steel bridges, and the applicability has been partially verified. However, there have been few research studies on the fatigue performance of old steel bridges after reinforcement, particularly because it is difficult to identify and monitor the fatigue cracks hidden behind reinforced plates. In this research, based on the fatigue test of the full-length specimens of steel truss bridge transverse longitudinal beam joints, combined with finite element software, a three-dimensional simulation model of beam joints with 230 mm cracks through the web before and after reinforcement is established. The stress field parameter changes at the crack tip and the stress redistribution law after reinforcement are studied, and the effectiveness of bolted steel plate reinforcement is evaluated. The prediction of the new crack nucleation location and the fatigue weakness details is of great significance for the intelligent sensing and monitoring of fatigue damage in the later operation of steel bridges.

2. EXPERIMENTAL INTRODUCTION AND MODEL BUILDING

2.1. Test specimen

Bolted steel plate reinforcement has the following advantages compared with welding, rivets, pasting steel plates, etc.: higher bearing capacity; stress concentration is improved, and the fatigue resistance of the connector is improved; construction speed is fast, installation is easy, and replacement is flexible, the steel bridge was reinforced with bolted steel plates in 2017. According to the maximum crack detected by the real bridge in the subject study, five full-size test specimens of a steel cross beam joint are designed in this experiment [2], the specimens are 2.95 meters long and are the point specimens at the design time of the original bridge (without cracks or reinforcement), numbered T1, as shown in Figure 1. There are two models with cracks before reinforcement, numbered T2 and T3, as shown in Figure 2a and 2b. There are two models with cracks strengthened, numbered T4 and T5, as shown in Figure 3.

2.2. Measured points

Each specimen has strain gauges affixed at key points according to the results of the numerical simulation, as shown in Figure 4. The strain data are monitored and collected at the same time and space during the test.

2.3. Finite element model

As shown in Figure 5, the finite element models of the cross beam joint are established before and after reinforcement with cracks, wherein solid Solid187 element is used for the beam and solid Solid186 element is used for the crack area.

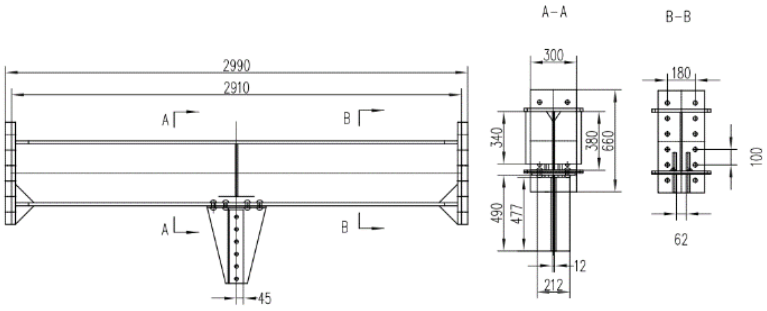

Figure 1. Test specimen without cracks before reinforcement.

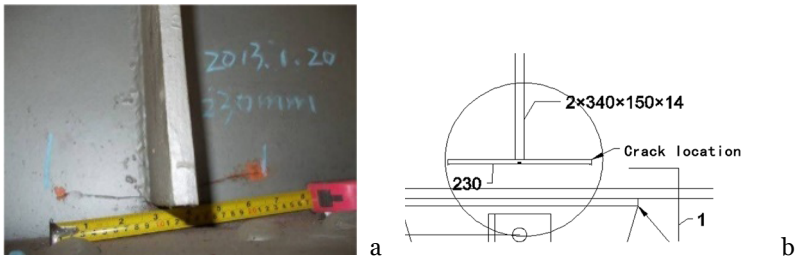

Figure 2. a) Measured crack size, b) Simulated crack.

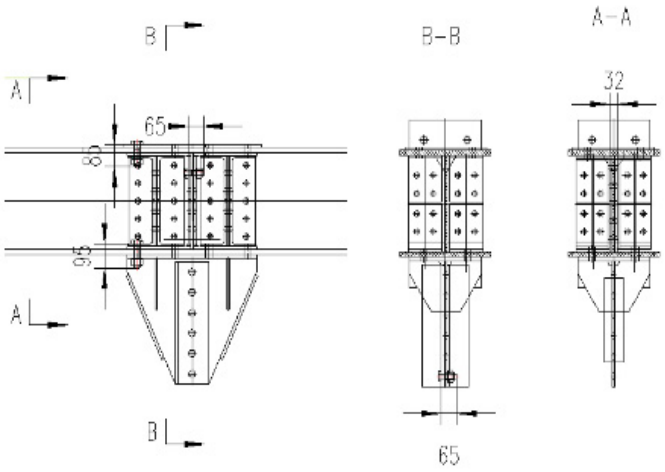

Figure 3. Specimen after reinforcement.

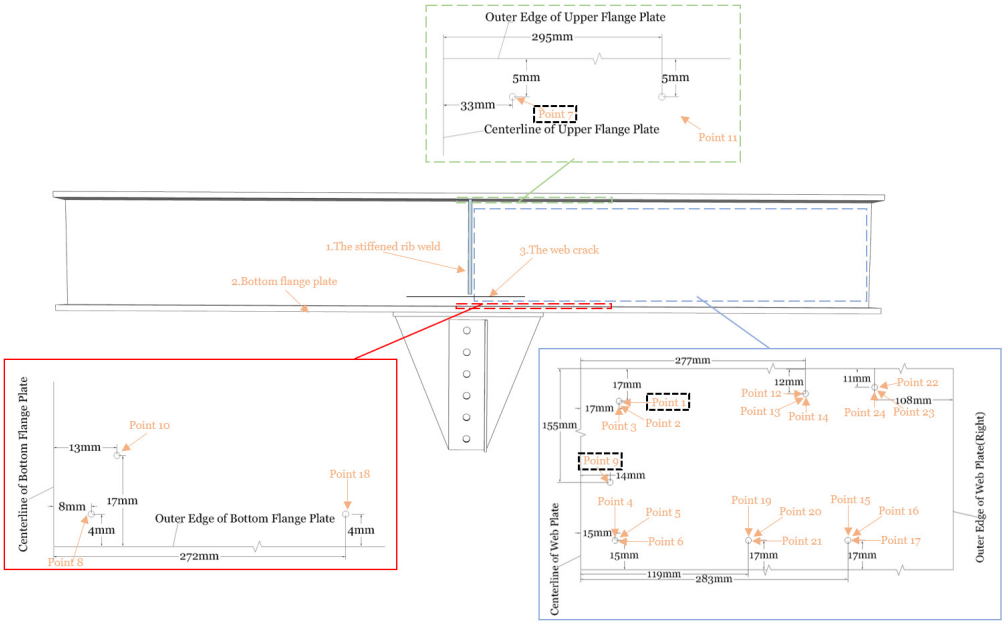

Figure 4. Arrangement of the measuring points.

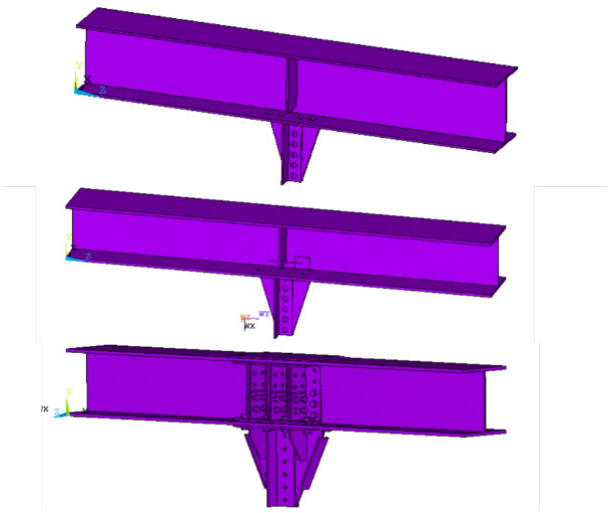

Figure 5. 3Dfinite element model.

The crack tip is meshed with singular finite elements, as shown in Figure 6.

A contact surface is set between the bolt and the connected member for simulation. Both ends of the beam model are boundary constraints, and only the longitudinal beam bearing area at the upper center of the beam is simulated under pressure, which makes the model conform to the actual working conditions and constraints of the test.

3. THE DATA AND NUMERICAL SIMULATION RESULTS

3.1. Stress analysis

In the fatigue test carried out on beam specimen T1, the maximum fatigue load is the sinusoidal constant amplitude load of 80 kN-880 kN, and the frequency is 2.5 Hz.

The data for the loading test are compared with the stress data of the corresponding measuring points calculated with the numerical simulation of the finite element model. The data for typical measuring points 1, 7, and 9 are selected for comparison, as shown in Table 1.

By comparing the data in Table 1, it can be found that there is little difference between the experimental data and the simulated data, and most of the data are within the error tolerance range, which indicates that the numerical simulation model has good accuracy.

3.2. Three-dimensional stress of crack tip

3.2.1. Three-dimensional stress distribution

The maximum amplitude of cyclic load is 80,000kg applying to the center of the beam (y, gravity direction), combined with the results of the test and the numerical simulation analysis, the three-dimensional stress states in the areas with large amplitudes of the fatigue stress, near the web crack, the lower flange plate, and the stiffening rib weld (as shown in Figure 4) are analyzed in depth.

1) Web with a crack

In the web crack area, the stress is concentrated on the crack tip. Figure 7 shows the stress cloud diagram of the maximum principal tensile stress S1 corresponding to the crack length of 230 mm. It can be seen from the figure that there is stress release in a certain range around the unreinforced cracking area. The precast crack area should be subjected to tensile stress, but it no longer bears the main tensile stress of the web and enters a state of compression. This part can be regarded as the section failure area of the web due to cracking. After reinforcement, the stress release in a certain range around the crack area becomes smaller,

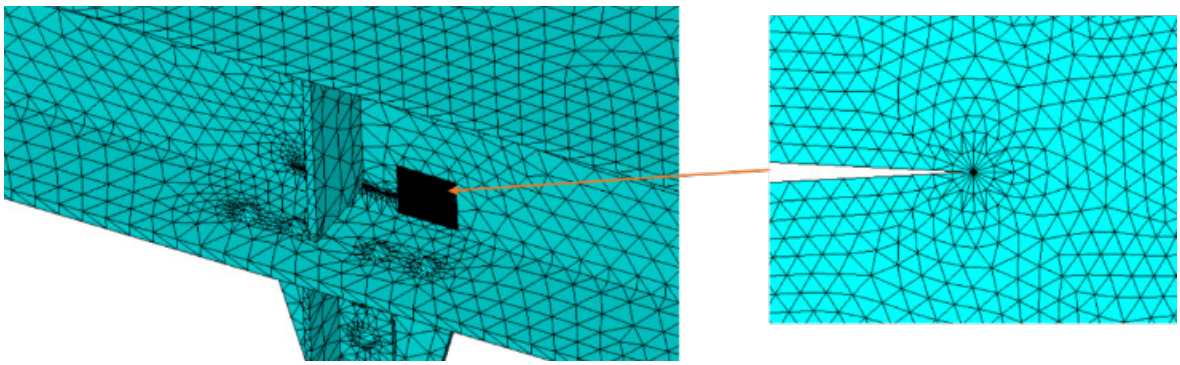

Figure 6. Singular elements near crack front.

Table 1. Comparisons between tested data and numerical data.

	Measuring point 1		contrast %	Measuring point 7		contrast %	Measuring point 9		contrast %
Load (t)	The experimental data (MPa)	Simulated data (MPa)		The experimental data (MPa)	Simulated data (MPa)		The experimental data (MPa)	Simulated data (MPa)	
10	-13.79	-11.05	19.85	-8.70	-8.24	5.23	-5.92	-5.99	1.11
20	-22.94	-22.08	3.73	-17.00	-17.11	0.65	-12.63	-12.70	0.55
30	-31.84	-33.12	4.00	-31.66	-30.04	5.11	-18.25	-18.52	1.49
40	-41.65	-44.00	5.64	-48.24	-44.17	8.44	-23.42	-23.18	1.05

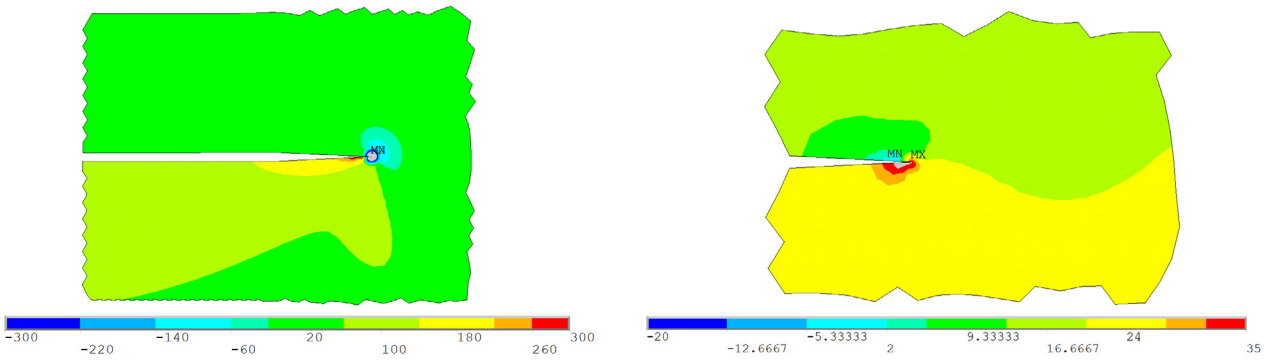

Figure 7. Stress concentration near the crack front before reinforcement (left) and after reinforcement (right).

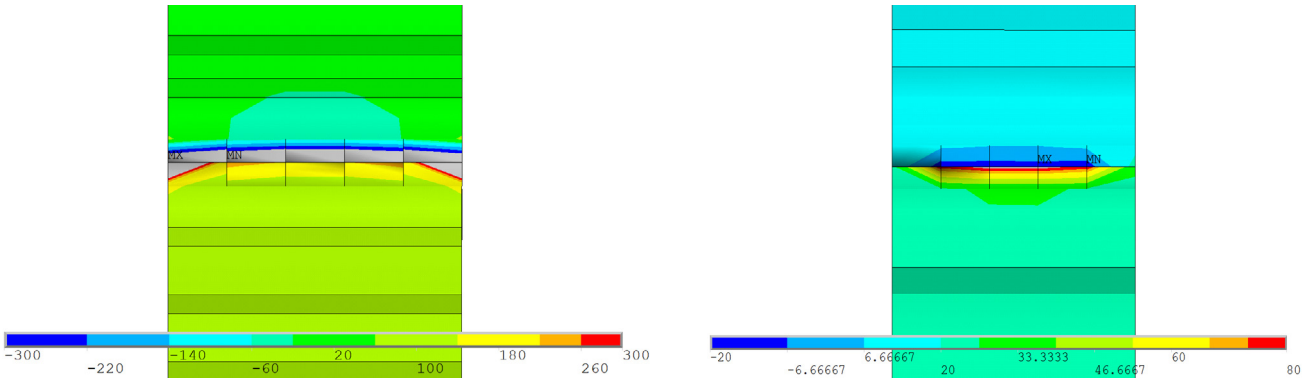

Figure 8. Distribution of primay tensile stress S1 in Z-axis for unreinforced (left) and reinforced (right) webs.

and the area below the crack can still help the main beam to bear tensile stress.

Figure 8 shows the distribution cloud diagram of the principal tensile stress S1 in the direction of the web thickness before and after reinforcement. It can be seen from this figure that the three-dimensional stress at the crack tip tends to increase from the center to both ends in the thickness direction. The stress cloud diagram shows that the compressive stress value on the web surface is significantly smaller than that in the middle of the web, which indicates that the three-dimensional stress has a great inhomogeneity along the thickness direction, and this inhomogeneity causes a large stress difference at the front of the crack. Under the condition of this test, the stress on the outside of the unreinforced web is relatively large, and the propagation rate is also large. Therefore, the inconsistency between the crack surface and the internal propagation front causes new tip cracks in the web. The stress picture shows that the compressive stress on the web surface is obviously smaller than that in the middle of the web. In the reinforced state, the inhomogeneity of the three-dimensional stress along the plate thickness direction is greatly improved, and the crack growth rate on the outer side of the web is alleviated, which can effectively reduce the crack growth.

The three-dimensional stress data at the crack tip are shown in Table 2, which shows that the stress in the direction of web thickness conforms to the empirical formula of Sz=m(Sx+Sy)(23), In the steel truss bridge girder web reinforcement studied in this research, the parameter m is 0.05.

2) Bottom flange plate

The distribution of the main tensile stress S1 of the lower flange plate is shown in Figure 9. It can be seen that the unreinforced beam has large tensile stress at the weld between the beam and the bottom plate, with an obvious stress concentration. The three-dimensional stress is symmetrically distributed at the edge of the bottom plate and reaches a maximum in the center. However, there is large tensile stress at the connection between the bolt hole of the lower flange plate and the bottom steel plate of the reinforced beam, with an obvious stress concentration. The three-dimensional stress is symmetrical at the edge of the lower flange plate, indicating that cracks can easily appear at the edge of the bolt hole and expand to the edge.

Table 2. The-dimensional stress relationship table at crack tip.

	Node	Sx	Sy	Sz	m=Sz/ (Sx+Sy)
Unreinforced	300731	-201.68	-198.18	18.53	0.05
	300733	-201.89	-198.25	18.48	0.05
Reinforced	1500798	20.56	-1.29	1.04	0.05
	1500801	12.08	0.36	-0.56	0.05

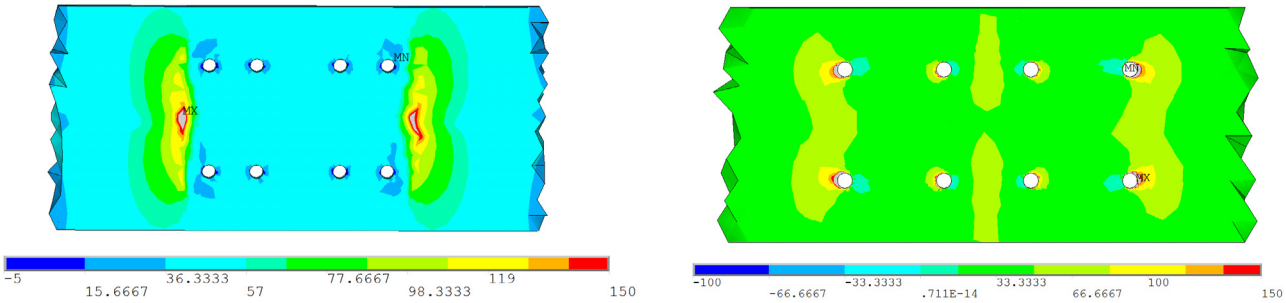

Figure 9. Distribution of primay tensile stress S1 of unreinforced (left) and reinforced (right) for bottom flange plates.

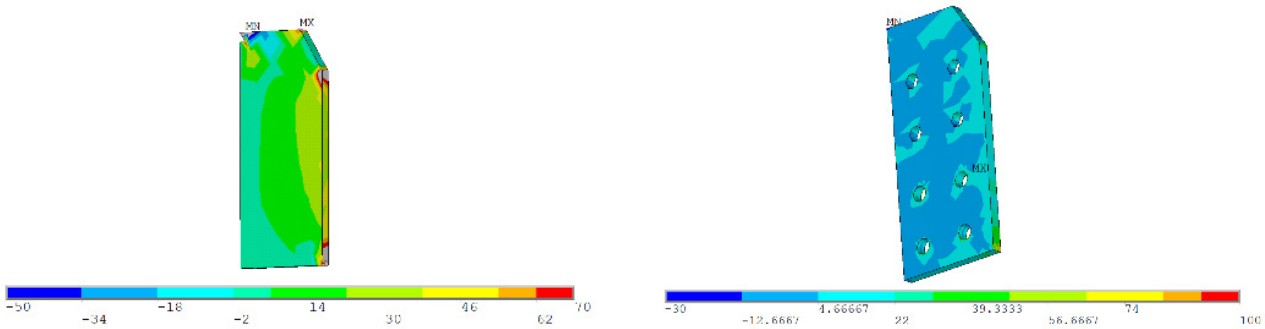

Figure 10. Distribution of primary tensile stress S1 at weld joint for unreinforced (left) and reinforced (right) rib.

3) Weld of stiffened rib plate

The stress diagram of the three-dimensional stress at the welding seam of the stiffened rib along the height direction (Y direction) is shown in Figure 10. According to the figure, the stress concentration phenomenon of the unreinforced beam near the welding seam in the height direction of the stiffened rib is prominent, there is large tensile stress at the welding seam at the bottom of the stiffened rib, and new cracks can easily appear at the maximum stress. After reinforcement, the stress concentration near the weld in the height direction of the stiffened ribs is weakened, and it is more difficult to crack the weld seams than those of the unstrengthened ribs.

3.2.2. Analysis of test results

The fatigue failure of the specimen is shown in Figure 11. In the figure, T1 is the beam without a prefabricated crack. The crack occurs at the joint of the stiffening rib weld and the rivet of the lower flange plate, as shown in Figure 11a. The earliest weld crack appears under the stiffening plate in the vertical direction, and the length of the fracture is about 60 mm. At the same time, cracks appear in the central section of the bolt hole of the lower flange plate. With the fatigue load cycling until the final full section fracture of the lower flange plate, the crack length is 73 mm. T2 and T3 are unreinforced prefabricated 230 mm crack beams with cracks occurring at the lower flange

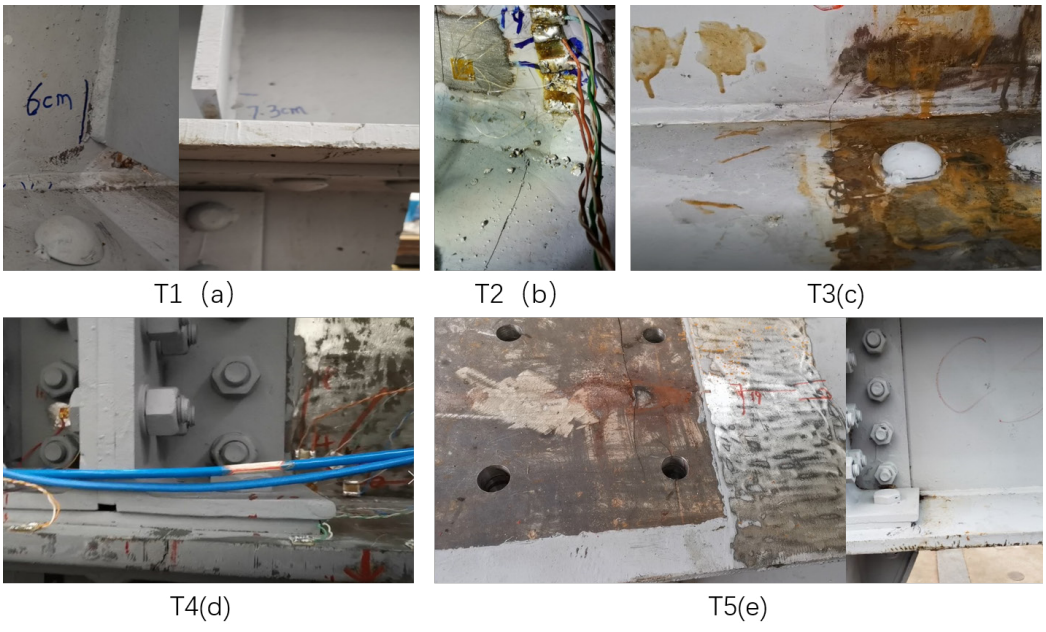

Figure 11. Fatigue failure cracks of specimens.

Table 3. Comparison of beam stress before and after reinforcement

	Stress	Before reinforcement (MPa)	After reinforcement (MPa)	The stress amplitude is reduced (%)
Web crack tip	*Sx*	-131.28	-25.38	80.67
	Sy	-256.97	-3.13	98.78
	Sz	-61.29	-2.12	96.54
Stiffened rib weld	*Sx*	96.58	34.22	64.57
	Sy	-15.96	-1.44	90.99
	Sz	-91.41	-44.50	51.32
Bottom flange plate	*Sx*	19.87	5.02	74.73
	Sy	0.11	0.04	60.00
	Sz	-0.12	-0.03	71.90

plate, as shown in Figure 11b and 11c, with cracks of 24 mm, 18 mm, and 2 mm. T4 and T5 are reinforced prefabricated 230 mm crack beams, and the cracks occur at the connection between the lower flange plate and the bolt and the lower flange plate attached to the steel plate, as shown in Figure 11d and 11e.

It can be seen that the failure crack location in the fatigue test is in good agreement with the crack initiation location predicted by the numerical simulation.

4. COMPARATIVE ANALYSIS BEFORE AND AFTER REINFORCEMENT

The maximum amplitude of cyclic load is 40,000kg applying to the center of the beam (y, gravity direction). The vertical stress amplitude of the web crack tip, the stiffener plate weld and the bottom flange plate before and after reinforcement are compared. It can be seen from Table 3 that the vertical stress in the joint is reduced after reinforcement for web and stiffener: Sy=-3.13MPa at the web crack tip, compared with the web crack tip Sy=-256.97MPa before retrofit, there is a reduction of 98.74%, the vertical stress amplitude of the crack tip was reduced observably. For the stiffened rib weld, Sy=-1.44MPa, compared with the stiffened rib weld Sy=-15.96MPa before retrofit, there is a reduction of 90.99%, effectively preventing the weld from shearing and cracking due to vertical force; For the bottom flange plate Sy=0.04MPa, compared with the bottom flange Sy=-0.11MPa before retrofit, there is a reduction of 60.00% and the tensile deflection of the lower flange plate is reduced. those results show that the reinforcement effect of the bolted steel plate is good, and the strength meets the requirements of bridge structure, especially for crack tip origin and stiffener weld. Due to the placement of multiple steel plates on both sides and fixed with high-strength bolts, the out-of-surface deformation amplitude of the web and the stiffener are reduced, and the stress amplitude is effectively reduced.

5. CONCLUSION

In this research, the full-size test of a steel bridge beam joint is carried out, and the stress variation of five test beams is analyzed, processed, and compared with the theoretical simulation data, which verifies the availability of the model. Based on the analysis of the three-dimensional stress amplitude field of the measured points, test data, and simulated data, the possible fatigue detail position of the cracks after reinforcement is predicted, and the stress estimation parameters and the distribution law of the fatigue stress amplitude are given for the web thickness direction of the steel beams.

The results for the fatigue test and the numerical simulation of the steel beam joints before and after reinforcement show that the following:

1) The structure after reinforcement is complex, and once damage occurs, multiple cracks may appear at multiple weak points. The traditional single crack growth mode cannot simulate the overall damage state of the real structure. There are several weak details in the final failure of the specimen (Figure 4). After the reinforcement of the tethered steel plate, the cracks preferentially appear below the web and near the center of the bolt hole of the lower flange plate. With the increase of the damage in the later stage, the lower end of the web stiffening rib weld and the outer edge of the plate attached to the lower flange plate also has a significant stress concentration. The monitoring system can set the monitoring and measuring points in advance at the weak details mentioned above, so the fatigue damage of the steel bridge in the later stage of reinforcement operation can be intelligently sensed.
2) The results of the 3D finite element numerical model presented in this study are in good agreement with the measured data and can be used in research on fracture mechanical properties and crack propagation rules.
3) The empirical formula parameter m[1] is approximately 0.05.

4) The reinforcement improves the local stress distribution of the beam joints, reduces the fatigue stress range in the reinforcement area obviously, and slows down the growth of the cracks. However, for the fatigue load with a large stress amplitude, the beam will create new cracks at new weak positions, and the damage will continue to accumulate and develop.

REFERENCES

(1) Dai Li, Liu Qiang, Ma Ke Zheng & Tan Jinhua (2021). Full-length fatigue test of cracked beam joints in steel truss Bridges. *Journal of Wuhan University of Technology*, Traffic Science and Engineering Edition, (02), 308-311.
(2) Ju Xiao-chen, Tian Yue, Pan Yong-jie, ZHAO Xin-xin (2015). Research on the prediction method of fatigue crack propagation behavior in steel Bridges. *Bridge Construction* (02), 53-57.

(3) Gao Wei, Zhan Ang & Zhou Jiang (2011). Force model for predicting fatigue life of joint plate of steel plate girder bridge. *Journal of Shenyang Jianzhu University*, Natural Science Edition, (03), 503-507.
(4) Qu Yu (2018). The local orthotropic steel bridge panel fatigue mechanism research. Ph.D. Dissertation, Chongqing Jiaotong University. https://kns.cnki.net/KCMS/detail/detail.aspx?dbname=CDFDLAST2019&filename=1018 149698.nh.
(5) Wang Chun-Sheng, Zhai Mu-Sai, Tang You-Ming, Chen Wei-Zhen & Qu Tian-Yu (2017). Numerical fracture mechanics simulation of coupled fatigue crack propagation mechanism in steel bridge panels. *China Journal of Highway and Transport* (03), 82-95. http://doi.org/10.19721/j.cnki.1001-7372.2017.03.009.
(6) Zhu Jin-song, Guo Yao-hua (2014). Fatigue crack propagation mechanism and numerical simulation of orthotropic steel bridge panels. *Vibration and impact*, (14), 47 + 40-71.
(7) Huang Yun, Zhang Qinghua, Yu Jia, Guo Yawen & Bu Yizhi (2019). Fatigue evaluation and crack propagation of steel bridge panels and longitudinal ribs. *Journal of Southwest Jiaotong University*, (02), 260-268.
(8) Liu Yiming, Zhang Qinghua, Cui Chuang & Bu Yizhi. (2016). Numerical simulation of three-dimensional fatigue crack propagation in orthotropic steel bridge panels. *China Journal of Highway and Transport*, (07), 89-95. http://doi.org/10.19721/j.cnki.1001-7372.2016.07.011.
(9) Wei-zhen Chen, G.A lbrecht, D.K osteas. (2001). Fatigue life prediction of welded steel bridge members. *Journal of Tongji University*, Natural Science Edition, (01),45-49.
(10) Zhang Ning, YU Kai, CUI Chuang & Zhang Qinghua. Cross-scale fatigue damage assessment method for steel bridge panels of long span Bridges. *Journal of Civil and Environmental Engineering*.
(11) Lv Zhilin, Jiang Xu, Qiang Xuhong, Wang Xiaojian (2021). Fatigue test study on local model of diaphragm of orthotropic steel bridge panel. *Structural Engineer,* (6), 163-171.
(12) Wang, T., Bin, J., Renaud, G., Liao, M., Lu, G., & Liu, Z. (2022). Probabilistic method for fatigue crack growth prediction with hybrid prior. *International Journal of Fatigue*, *157*, 106686.
(13) Nagarajappa, N., Malipatil, S. G., Majila, A. N., Fernando, D. C., Manjuprasad, M., & Manjunatha, C. M. (2022). Fatigue Crack Growth Prediction in a Nickel-Base Superalloy Under Spectrum Loads Using FRANC3D. *Transactions of the Indian National Academy of Engineering*, *7*(2), 533-540.
(14) Li, M., Liu, X., Li, Z., & Zhang, Y. (2021). Fatigue crack growth prediction model under variable amplitude loading conditions. *International Journal of Damage Mechanics*, *30*(9), 1315-1326.
(15) Xiao, B., Robertson, T., Huang, X., & Kearsey, R. (2020). Fracture performance and crack growth prediction of SPS TBCs in isothermal experiments by crack numbering density. *Ceramics International*, *46*(3), 2682-2692.
(16) Fuller, R. W., Simsiriwong, J., & Shamsaei, N. (2020). Crack growth prediction for irradiated stainless steels under the combined fatigue-creep loading. *Theoretical and Applied Fracture Mechanics*, *109*, 102759.
(17) Cheng, A., Chen, N. Z., Pu, Y., & Yu, J. (2020). Fatigue crack growth prediction for small-scale yielding (SSY) and non-SSY conditions. *International Journal of Fatigue*, *139*, 105768.
(18) Cheng, A., Chen, N. Z., & Pu, Y. (2019). An energy principles based model for fatigue crack growth prediction. *International Journal of Fatigue*, *128*, 105198.
(19) Qiu, Z., & Zhu, J. (2019). The perturbation series method based on the logarithm equation for fatigue crack growth prediction. *Theoretical and Applied Fracture Mechanics*, *103*, 102239.
(20) Husnain, M. N. M., Akramin, M. R. M., & Chuan, Z. L. (2019). Surface crack growth prediction under fatigue load using the S-version Finite Element Model (S-FEM). In *IOP Conference Series: Materials Science and Engineering (*IOP Publishing), 469(1), 012011.
(21) Sundqvist, J., Kaplan, A. F., Granström, J., Sundin, K. G., Keskitalo, M., Mäntyjärvi, K., & Ren, X. (2015). Identifying residual stresses in laser welds by fatigue crack growth acceleration measurement. *Journal of Laser Applications*, *27*(4), 042002.
(22) Azar, A. S., Svensson, L. E., & Nyhus, B. (2015). Effect of crystal orientation and texture on fatigue crack evolution in high strength steel welds. *International Journal of Fatigue*, *77*, 95-104.
(23) Wang Yuanqing (1995). Brittle failure tendency of steel structural members in high stress concentration zone. *Engineering Mechanics* (03).